Optimization of Element Positions in Linear Optical Phased Arrays for Broad Beam Steering Operation

Bruna D. P. Souza, Ivan Aldaya, Julián L. Pita, Marcelo L. F. Abbade, Paulo F. Jarschel, and Rafael A. Penchel

***Abstract*— Optical phased arrays (OPA) are used to improve the radiation characteristics of single-element antennas and allow dynamic control of the radiation pattern. However, the manufacturing constraints of complementary metal oxide semiconductor (CMOS) platform limits the minimum inter-element separation to more than half of the operation wavelength, which in uniform arrays results in the appearance of high intensity secondary lobes, called grating lobes. In this work, we optimize the position of the elements in a non-uniform linear OPA for different beam steering angles. The preliminary results showed that the optimal position of the elements depends on the desired beam steering angle.**

***Keywords*— Photonic antenna, optical phased array, grating lobes, LIDAR.**

I. Introduction

In recent years, photonic antennas (PAs) have been extensively studied due to their critical role in applications ranging from spectroscopy [1] and free-space communications [2] to *Laser Imaging Detection and Ranging* (LIDAR) [3]. The first PAs were built with a metallic structure to support plasmon resonances [4]. However, metallic PAs present high ohmic losses and, consequently, low power efficiency. In order to overcome this drawaback, all-dielectric antennas were developed [5]. In particular, complementary metal oxide semiconductor (CMOS)-compatible silicon PAs have emerged as a high potential solution because, on the one hand, they take advantage of the mature manufacturing infrastructure and, on the other hand, can be naturally integrated with other constitutive blocks [6].

Similar to the RF domain, arrangement of multiple identical PAs in optical phased arrays (OPAs) have been proposed as a flexible solution not only to improve the radiation characteristics but also to allow dynamic control of the radiation pattern by controlling the feeding of the elements [7]. Unfortunately, the footprint of the elements in integrated OPAs is usually larger than the operation wavelength, λ and, therefore, it poses a limitation to the minimum inter-element separation [8]. In addition, in order to meet the fabrication constraints and avoid evanescent coupling between the waveguides, the design of the feeding network imposes an even larger inter-element minimum separation [9]. Therefore, the distance between elements generally exceeds various wavelengths, resulting in a so-called sparse array. When the elements are uniformly distributed, the large separation between them leads to the appearance of high intensity secondary lobes that are commonly denominated as grating lobes [10]. In this case, the side lobe level (SLL) defined as the ratio between the main lobe and the more prominent side lobe. As shown in [11], the strength of these grating lobes is particularly high when the separation increases and beam steering is implemented. Reducing the amplitude of these grating lobes is then critical in sensing and communications application to avoid interference, crosstalk, and possible security faults [3], [12], [13].

The optimization of linear arrays, although simpler than that of planar configurations, remains of interest because some OPAs rely on in-plane radiators, such as guides or tapers, that are arranged following a linear geometry. Figure 1 shows an example of an in-plane OPA. In this case, beam steering is performed along the direction of the subtract plane, which we will refer as the azimuthal plane. To reduce the SLL of linear OPAs, a well-known solution is the use of arrays with non-uniform separations between the elements. This issue has been addressed by several computational methods. For instance, in [14], the particle swarm algorithm is used to determine the positions of the elements, whereas in [15]

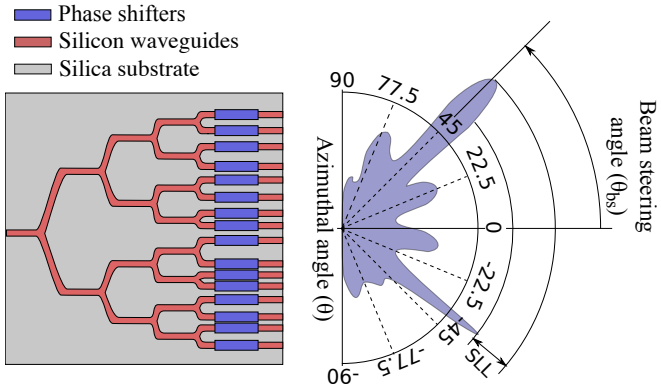

Fig. 1. Top view of the in-plane OPA with optimized nonuniform inter-element spacing alongside the cut in the azimuthal plane of the radiation pattern.

Bruna D. P. Souza, Ivan Aldaya, Marcelo L. F. Abbade, and Rafael Abrantes Penchel, Campus de São João de Boa Vista, Universidade Estadual Paulista (UNESP), São João da Boa Vista-SP, e-mail: bdpsouza@gmail.com, {ivan.aldaya, marcelo.abbade, rafael.penchel}@unesp.br; Julián L. Pita, Faculdade de Engenharia Elétrica e Computação, Universidade Estadual de Campinas (UNICAMP), Campinas-SP, e-mail: jlpitar@gmail.com. Paulo F. Jarschel, Instituto de Física Gleb Wataghin, Universidade Estadual de Campinas (UNICAMP), Campinas-SP, e-mail: pfjarschel@gmail.com.

genetic algorithm is used. However, even if in [13] the effect of beam steering is considered, the optimization in both works is limited to broadside configuration. Thus, although [13] and other works [10][11] shows that the SLL degrades as the beam steering angle increases, it is still not clear how the dependency of the SLL on the beam steering angle θ_{bs} is affected when the element positions are optimized considering different design beam steering angles θ_{des}.

In the present work, we optimized the positions of the antenna elements in a linear OPA for different beam steering angles, in the range between 0º and 45º. As the intermediate optimizations between the chosen angle range followed the same trend, for clarity we present here the results for 0º, 22.5º, and 45º. Several optimization methods could be used to achieve this goal. In this first work on the subject, we chose to use the differential evolution (DE) as an optimization tool because of its good trade-off between complexity and performance. In fact, as further explained, we found that DE provides some important insights on the description of side lobes evolution. Moreover, DE results can possibly be used as a benchmark for optimization methods considered in future work. The algorithm was developed in high level language, in the Matlab software. It is important to note that we did not calculate the SLL of the whole OPA but of its array factor (AF). This approach is often adopted because it makes the optimization process to be independent of the element radiation pattern. In addition, the calculation of the SLL of the AF is a good approximation of the whole OPA when the element radiation diagram has a wide main lobe. The found configurations revealed that the optimum position of the elements depends on the maximum beam steering angle. The remainder if this paper is organized as follows. In Section II we describe the DE optimization procedure. Simulation results are approached in Section III. Finally, our conclusion is presented in Section IV.

II. Optimization of Element Positions Using Differential Evolution

DE is a well-known multi-objective optimization method developed by Rainer Storn and Kenneth Price that has been applied in areas as diverse as economy [16] and electrical engineering [17]. This algorithm emulates the natural evolution of live species. At each iteration, a new generation of tentative solutions is created and the suitability of each new individual, corresponding to the positions of the nonuniform element positions, is assessed employing a suitable cost function to be optimized. In our case, the cost function is the SLL, which requires the previous calculation of the AF of an N-element array with its elements located at z_n. Applying the superposition principle, we can find an expression for the AF [18]:

$$AF(\theta) = \sum_{n=1}^{N} \exp(jk\ z_n \cos\theta + \beta_n), \tag{1}$$

where k is the wavelength vector, and the β_n are the feeding phases that depend on the value of θ_{des} according to:

$$\beta_n = -k\ z_n \cos\theta_{des} \quad 1 \leq n \leq N. \tag{2}$$

TABLE I
Employed OPA and DE algorithm parameters.

OPA parameters	
Parameter	**Value**
Number of antenna elements	16
Average distance	1λ
Minimum distance	0.5λ
Design beam steering angle	0º, 22.5º, 45º
DE parameters	
Parameter	**Value**
Population size	50
Iterations	1,000
Repetitions	10
Crossover probability	0.1
Scaling factor range	[0.2,0.8]

Once the AF is calculated, we need to find the amplitudes of the main lobe, $|AF(\theta_{ML})|$ and of the highest power secondary lobe $|AF(\theta_{ML})|$. The SLL, our cost function, can then be calculated as:

$$SLL = \frac{|AF(\theta_{ML})|^2}{|AF(\theta_{SL})|^2}. \tag{3}$$

For each generation, the best individuals in terms of the cost function are combined to create a new generation with improved performance. The algorithm terminates either when the best individual meets the required performance or when the maximum number of iteration specified by the user is reached.

One of the features of DE is that its performance is highly dependent on the genetic wealth of the initial population. In other words, how different the elements of the first generation are. In order to improve it, there are different approaches that can be adopted: i) use a larger number of individuals for each generation; ii) use a selective set of individuals, discarding elements that are similar and that do not add much genetic variation; and iii) use different random initial generations and perform several parallel DE processes. In this work we chose the last alternative as it is simple to implement and offers a

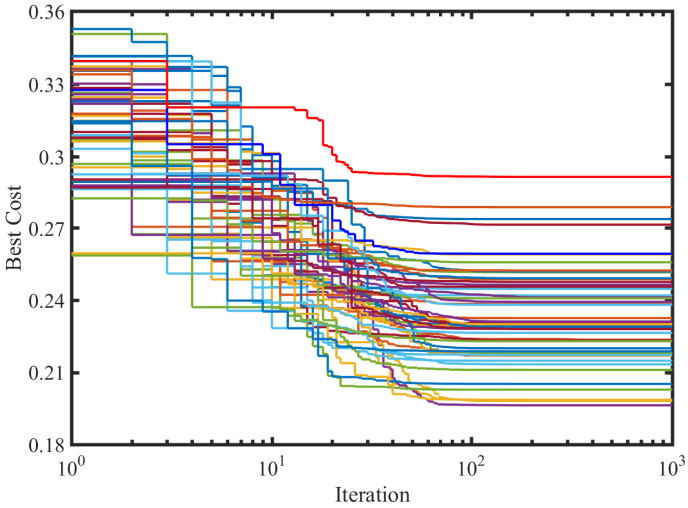

Fig. 2. Best cost functions, SLLs, for different initial populations as a function of the iteration.

good performance.

Table I shows the parameters of the OPA to be optimized and of the employed DE algorithm. The parameters of the OPA, obviously depend on the particular application and its constraints, whereas we are relatively free to select the parameters of the optimization algorithm, which typically require some refinement. In order to justify the configuration adopted for the optimization, we can look at the evolution of the best cost function at each generation, which is shown in Fig. 2 for a $\theta_{des} = 45^{\text{o}}$. In the figure, each line represents the best cost function, for a particular initial population. As expected, the best SLLs decrease until it converges to values that depend on the particular initial population. Regarding the number of iterations, it can be see that after the iteration 100, there is little improvement, so by limiting the maximum iteration number to 1,000 we are exaggerating on the side of caution. The number of repetitions also seems to be enough to achieve a good tradeoff between performance and computational cost.

III. Results

Figure 3(a) shows the SLL in logarithmic scale as a function of the beam steering angle θ_{bs} of non-uniformly distributed 16-element arrays for three different values of θ_{des}: 0^{o}, 22.5^{o}, and 45^{o}. In the same figure, we superimposed the optimized configuration for each θ_{des}, represented by the points arranged in the horizontal direction that, as can be seen, are different for each θ_{des}. Comparing the SLL curves for the different values of θ_{des}, it is clear that for low narrow beam steering, the OPA designed for 0^{o} outperforms the other two. As θ_{des} increases, however, the SLL shown by the OPA designed for 0^{o} rapidly deteriorates and the other two OPA show better performance. If we consider a θ_{bs} range up to 22.5^{o}, the θ_{des} of the second OPA, the best performance is achieved by the array designed for this θ_{des}. For θ_{bs} values larger than $\theta_{des} = 22.5^{\text{o}}$ the second OPA also shows worse SLL. Finally, for θ_{bs} angles between 22.5^{o} and 45^{o}, the OPA optimized for θ_{des} shows the better performance. For even larger θ_{bs} angles, it is expected that the third OPA, optimized for $\theta_{des} = 45^{\text{o}}$, to present poorer performance and would require further optimization. We did not explore this because we considered that a beam steering covering from -45° to +45° satisfies the requirements of most applications.

In order to verify the SLL curves and understand the their stair-like shape, in Fig. 3(b) we show the contourmaps of the AF amplitude for the three optimized arrays in terms of the azimuthal angle θ and beam steering angle θ_{bs}. In Fig. 3(b.i) the OPA was optimized for the 0^{o} steering angle, in Fig. 3(b.ii) for 22.5^{o} steering angle and in Fig. 3(b.iii) for 45^{o} steering angle. In all the three cases, the beam steering operation is clear by noting the main lobe shift. This main lobe has a maximum of 16, which corresponds to the number of radiating elements. For $\theta_{des} = 0^{\text{o}}$, a significant sidelobe emerges for low beam steering angles, and generates the fast degradation observed in Fig. 3(a). For the OPA designed for $\theta_{des} = 22.5^{\text{o}}$ shown in Fig. 3(b.ii), it can be observed that no significant sidelobe appears up to a beam steering corresponding to the designed beam steering angle. After this, the emergence of a sidelobe deteriorates the SLL of the OPA. The same behavior is obtained for the case of θ_{des} presented in Fig. 3(b.iii). That is, no sidelobes appear for beam steering angles smaller than the design angle of 45^{o}.

We can then conclude that the OPA has to be designed for the worst-case scenario, that is, for the largest beam steering angle. This induces a penalization for low beam steering angles but an improved performance over the whole beam steering range. For instance, when using a OPA optimized for $\theta_{des} = 45^{\text{o}}$, we have a penalization of ≈5.5 dB for $\theta_{bs} = 0^{\text{o}}$ with respect to the OPA designed for 0^{o}, but a SLL improvement of more than 10 dB for large θ_{bs} values. As additional consequence, to cover the whole circumference (360^{o}), we can improve the overall SLL by increasing the number of sectors in which the circumference is divided. For instance, if we consider four sectors, the SLL is ≈12 dB, whereas if we employ eight sectors, it turns to be reduced down to ≈14 dB.

IV. Conclusions

In this work we applied DE to optimize linear OPAs for different beam steering ranges, showing that the optimum elements positioning depends on the maximum beam steering angle. By optimizing for a large steering range, the SLL at low angles is penalized by the worst SLL over the whole range is improved. In the worst case scenario, that is, for an OPA design to 45^{o} steering angle, the SLL was improved by more than 10 dB with respect to the 0^{o} steering angle design situation. However, this optimization induced a penalty of approximately 5.5 dB for steering angles close to 0^{o}, which shows that each optimized arrangement is optimal in its projected operating angle. We also briefly discussed the relation between sectorization on the overall SLL, whereas the effect of the number of elements, the total array length and the minimum separation on the SLL is left as future work.

Acknowledgments

The authors thank the National Council for Scientific and Technological Development (CNPq, grant numbers 432303/2018-9 and 311035/2018-3) and the São Paulo Research Foundation (FAPESP, grant 2018/25339-4).

References

[1] L. Langguth, A. Szuba, S. A. Mann, E. C. Garnett, G. H. Koenderink, and A. F. Koenderink, "Nano-antenna enhanced two-focus fluorescence correlation spectroscopy," *Scientific Reports*, vol. 7, no. 1, p. 5985, 2017.

[2] A. Alù and N. Engheta, "Wireless at the nanoscale: optical interconnects using matched nanoantennas," *Physical Review Letters*, vol. 104, no. 21, p. 213902, 2010.

[3] C. T. Phare, M. C. Shin, J. Sharma, S. Ahasan, H. Krishnaswamy, and M. Lipson, "Silicon optical phased array with grating lobe-free beam formation over 180 degree field of view," in *CLEO: Science and Innovations*. Optical Society of America, 2018, pp. SM3I–2.

[4] G. W. Bryant, F. J. García de Abajo, and J. Aizpurua, "Mapping the plasmon resonances of metallic nanoantennas," *Nano Letters*, vol. 8, no. 2, pp. 631–636, 2008.

[5] A. E. Krasnok, A. E. Miroshnichenko, P. A. Belov, and Y. S. Kivshar, "All-dielectric optical nanoantennas," *Optics Express*, vol. 20, no. 18, pp. 20 599–20 604, 2012.

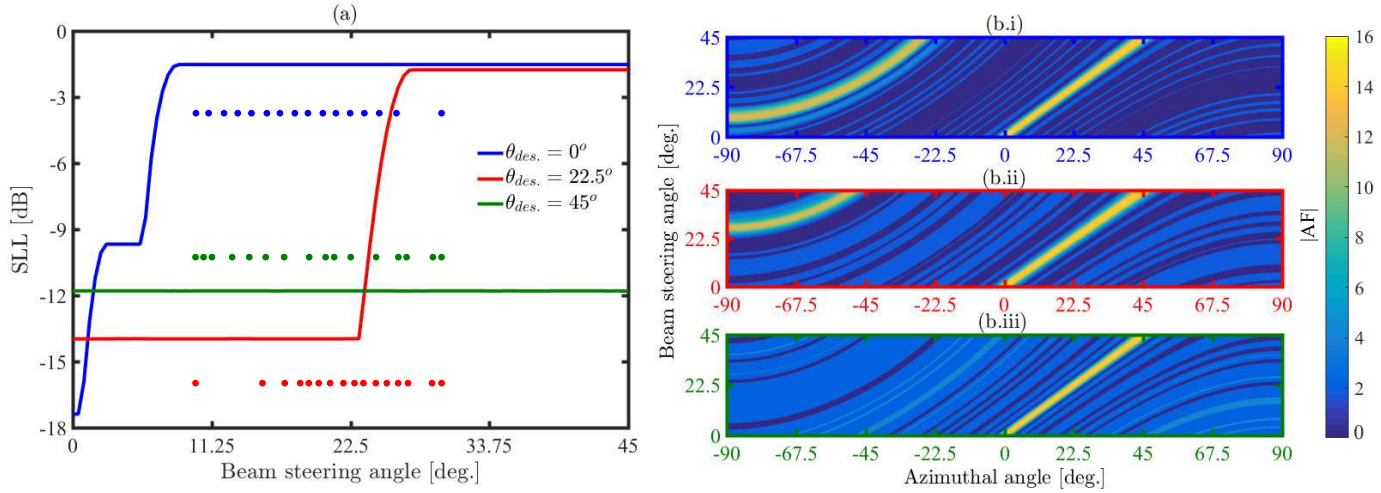

Fig. 3. (a) SLL in terms of beam steering angle for linear 16-element OPAs designed for beam steering of 0º, 22.5º, and 45º. The optimized position for each configuration is superimposed. (b) Magnitude of the AF for the optimized OPAs: (i) 0º, (ii) 22.5º and (iii) 45º.

[6] J. L. Pita, I. Aldaya, P. Dainese, H. E. Hernandez-Figueroa, and L. H. Gabrielli, "Design of a compact CMOS-compatible photonic antenna by topological optimization," *Optics Express*, vol. 26, no. 3, pp. 2435–2442, 2018.

[7] J.-H. Kim, J.-B. You, J.-H. Park, K. Yu, and H.-H. Park, "Design of nano-photonic phased-array antennas for wide-angle beam-steering," in *18th International Conference on Advanced Communication Technology (ICACT)*. IEEE, 2016, pp. 422–425.

[8] J. Pita, "CMOS-compatible compact photonic antennas / antenas fotônicas compactas compatíveis com a tecnologia CMOS," Ph.D. dissertation, 2018.

[9] J. L. Pita, I. Aldaya, O. J. Santana, P. Dainese, and L. H. Gabrielli, "Side-lobe level reduction in bio-inspired optical phased-array antennas," *Optics Express*, vol. 25, no. 24, pp. 30 105–30 114, 2017.

[10] Á. C. Aznar, J. R. Robert, J. M. R. Casals, L. J. Roca, S. B. Boris, and M. F. Bataller, *Antenas*. Univ. Politèc. de Catalunya, 2004, vol. 3.

[11] B. D. Pires de Souza, A. E. Ferreira Junior, F. Abbade, M. Luis, and I. Aldaya, "Side-lobe level reduction in 1D photonic array antennas," in *Sbfoton International Optics And Photonics Conference (sbfoton Iopc)*. Ieee, 2018, p. 4.

[12] J. L. Pita, P. C. Dainese, H. E. Hernandez-Figueroa, and L. H. Gabrielli, "Ultra-compact broadband dielectric antenna," in *CLEO: Science and Innovations*. Optical Society of America, 2016, pp. SM3G–7.

[13] B. D. P. de Souza, A. E. F. Junior, M. L. F. Abbade, and I. Aldaya, "Side-lobe level reduction in 1d photonic array antennas," in *2018 SBFoton International Optics and Photonics Conference (SBFoton IOPC)*. IEEE, 2018, pp. 1–4.

[14] M. M. Khodier and C. G. Christodoulou, "Linear array geometry synthesis with minimum sidelobe level and null control using particle swarm optimization," *IEEE Transactions on Antennas and Propagation*, vol. 53, no. 8, pp. 2674–2679, 2005.

[15] M. G. Bray, D. H. Werner, D. W. Boeringer, and D. W. Machuga, "Optimization of thinned aperiodic linear phased arrays using genetic algorithms to reduce grating lobes during scanning," *IEEE Transactions on Antennas and Propagation*, vol. 50, no. 12, pp. 1732–1742, 2002.

[16] L. Wu, Y. Wang, X. Yuan, and Z. Chen, "Multiobjective optimization of HEV fuel economy and emissions using the self-adaptive differential evolution algorithm," *IEEE Transactions on vehicular technology*, vol. 60, no. 6, pp. 2458–2470, 2011.

[17] A. Qing, *Differential evolution: fundamentals and applications in electrical engineering*. John Wiley & Sons, 2009.

[18] C. A. Balanis, *Antenna theory: analysis and design*. John wiley & sons, 2016.